UDC 621.396.962

MATHEMATICAL MODEL OF CURRENT TIME OF SIGNAL FROM SERIAL COMBINATION LINEAR-FREQUENCY AND QUADRATICALLY MODULATED FRAGMENTS

Kostyria O. O. – Dr. Sc., Senior Research, Leading Research Scientist, Ivan Kozhedub Kharkiv National Air Force University, Kharkiv, Ukraine.

Hryzo A. A. – PhD, Associate Professor, Head of the Research Laboratory, Ivan Kozhedub Kharkiv National Air Force University, Kharkiv, Ukraine.

Khudov H. V. – Dr. Sc., Professor, Head of Department, Ivan Kozhedub Kharkiv National Air Force University, Kharkiv, Ukraine.

Dodukh O. M. – PhD, Leading Research Scientist, Ivan Kozhedub Kharkiv National Air Force University, Kharkiv, Ukraine.

Solomonenko Y. S. – PhD, Deputy Head of the Faculty of Educational and Scientific Work, Ivan Kozhedub Kharkiv National Air Force University, Kharkiv, Ukraine.

ABSTRACT

Context. One of the methods of solving the actual scientific and technical problem of reducing the maximum level of side lobes of autocorrelation functions of radar signals is the use of nonlinear-frequency modulated signals. This rounds the signal spectrum, which is equivalent to the weight (window) processing of the signal in the time do-main and can be used in conjunction with it.

A number of studies of signals with non-linear frequency modulation, which include linearly-frequency modulated fragments, indicate that distortions of their frequency-phase structure occur at the junction of the fragments. These distortions, depending on the type of mathematical model of the signal – the current or shifted time, cause in the generated signal, respectively, a jump in the instantaneous frequency and the instantaneous phase or only the phase. The paper shows that jumps occur at the moments when the value of the derivative of the instantaneous phase changes at the end of the linearly-frequency modulated fragment. The instantaneous signal frequency, which is the first derivative of the instantaneous phase, has an interpretation of the rotation speed of the signal vector on the complex plane. The second derivative of the instantaneous phase of the signal is understood as the frequency modulation rate.

Distortion of these components leads to the appearance of an additional component in the linear term of the instantaneous phase, starting with the second fragment. Disregarding these frequency-phase (or only phase) distortions causes distortion of the spectrum of the resulting signal and, as a rule, leads to an increase in the maxi-mum level of the side lobes of its autocorrelation function. The features of using fragments with frequency modulation laws in complex signals, which have different numbers of derivatives of the instantaneous phase of the signal, were not considered in the known works, therefore this article is devoted to this issue.

Objective. The aim of the work is to develop a mathematical model of the current time of two-fragment nonlinear-frequency modulated signals with a sequential combination of linear-frequency and quadratically modulated fragments, which provides rounding of the signal spectrum in the region of high frequencies and reducing the maximum level of side lobes of the autocorrelation function and increasing the speed of its descent.

Method. Nonlinear-frequency modulated signals consisting of linearly-frequency and quadratically modulated fragments were studied in the work. Using differential analysis, the degree of influence of the highest derivative of the instantaneous phase on the frequency-phase structure of the signal was determined. Its changes were evaluated using time and spectral correlation analysis methods. The parameters of the resulting signal evaluated are phase and frequency jumps at the junction of fragments, the shape of the spectrum, the maximum level of the side lobes of the autocorrelation function and the speed of their descent.

Results. The article has further developed the theory of synthesis of nonlinear-frequency modulated signals. The theoretical contribution is to determine a new mechanism for the manifestation of frequency-phase distortion at the junction of fragments and its mathematical description. It was found that when switching from a linearly-frequency modulated fragment to a quadratically modulated frequency-phase distortion of the resulting signal, the third derivative of the instantaneous phase becomes, which, by analogy with the theory of motion of physical bodies, is an acceleration of frequency modulation. The presence of this derivative leads to the appearance of new components in the expression of the instantaneous frequency and phase of the signal. The compensation of these distortions provides a decrease in the maximum level of the side lobes by 5 dB and an increase in its descent rate by 8 dB/deck for the considered version of the non-linear-frequency modulated signal.

Conclusions. A new mathematical model of the current time has been developed for calculating the values of the instantaneous phase of a nonlinear-frequency modulated signal, the first fragment of which has linear, and the second – quadratic frequency modulation. The difference between this model and the known ones is the introduction of new components that provide compensation for frequency-phase distortions at the junction of fragments and in a fragment with quadratic frequency modulation. The obtained oscillogram, spectrum and autocorrelation function of one of the synthesized two-fragment signals correspond to the theoretical form, which indicates the adequacy and reliability of the proposed mathematical model.

KEYWORDS: mathematical model; linear and quadratic frequency modulation; maximum level of side lobes.

ABBREVIATIONS

ACF is an autocorrelation function;

SL is a side lobe;

MOP is a modulation on pulse or internal pulse frequency modulation;

WP is a weight processing;

DOI 10.15588/1607-3274-2024-2-3

ML is a main lobe;
RCS is a radar cross section;
QFM is a quadratic frequency modulation;
RSFM is a root-square frequency modulation;
LFM is a linear frequency modulation;
MM is a mathematical model;
MPSLL is a maximum peak side lobe level;
NLFM is a non-linear frequency modulation;
FMA is a frequency modulation acceleration;
PSLL is a peak side lobe level;
FM is a frequency modulation;
FMR is a frequency modulation rate.

NOMENCLATURE

C_1 is a integration constant;
$F(\cdot)$ is a functional dependency;
f_0 is a initial signal frequency, Hz;
$f_n(t)$ is a instantaneous frequency n-th fragment NLFM, Hz;
n=1, 2 is a serial number signal fragment LFM;
t is a current time, s;
T_n is a duration of the n-th signal fragment NLFM, s;
α_2 is a FMA n-th signal fragment NLFM, Hz/s^2;
β_n is a FMR n-th signal fragment NLFM, Hz/s;
Δf_n is a frequency deviation of the n-th signal fragment NLFM, Hz;
δf_{12} is a frequency jump when moving from 1-th signal fragment NLFM to 2-th, Hz;
$\delta\varphi_{12}$ is a phase jump when moving from 1-th до 2-th signal fragment NLFM, rad;
$\varphi(t)$ is a instantaneous phase of synthesized NLFM, rad;
$\varphi_n(t)$ is a instantaneous phase n-th signal fragment NLFM, rad.

INTRODUCTION

Modern methods and means of digital synthesis of radar signals open wide prospects for the formation of probing signals with improved spectral characteristics and correlation properties [1–7].

The combination of signals with different MOP laws and the synthesis of new types of signals of this type was restrained by the insufficient depth of the theoretical analysis of processes occurring at the moments of change of the FM law.

In works [8–10] on the example of NLFM signals with LFM fragments it is shown that frequency and phase jumps occur at their joints or only phases depending on the time representation of MM – in the current or shifted time. Approximation of the FM law to the S-shape provides a smoother rounding of the signal spectrum, which helps to reduce MPSLL. To achieve this, the authors [11–16] combined LFM with non-linear MOP in the lower and upper frequency regions of the NLFM signal. This method reduces MPSLL only for a limited number of parameter sets.

During the studies, it was found that frequency and phase jumps at the junction of LFM and QFM fragments were not previously considered and did not have a formalized description. The presence of such frequency-phase distortions leads to distortions in the temporal and spectral structure of the signal.

The development of an MM signal of the LFM-QFM type for the current time, which allows to take into account a new source of frequency-phase jumps and determine the consequences of these jumps, is devoted to this article. Such an MM two-fragment NLFM signal is selected to provide better visibility of the studies and their illustrative nature.

The object of study is the process of synthesis and optimal processing of two-fragment NLFM signals.

The subject of study is the NLFM MM signal, the first fragment of which has LFM, and the second – QFM.

The known sampling methods [2–23] are highly iterative and low speed, as well as characterized by the uncertainty of quality criteria of formed subsample.

The purpose of the work is to develop MM of the current time of two-phase NLFM signals with frequency-phase distortion compensation for the case when the first fragment has LFM, and the second – QFM. This rounds the signal spectrum in the high frequency region, thereby reducing MPSLL and increasing its decay rate.

1 PROBLEM STATEMENT

For further presentation of the material, we justify the feasibility of using the concepts of FMR and FMA. According to the general theory of radio oscillations, the full foray of the signal phase is interpreted as the area under the signal curve, and therefore the first derivative of the instantaneous phase is interpreted as the path that passes the end of the phase vector and this derivative is called the signal frequency. In the theory of motion of physical bodies, the derivative of the path is the speed, and in the presence of frequency modulation for the derivative of the frequency, the use of the concept of FMR instead of "scan speed", which is reasonably used in the English literature, is justified. Since the derivative of the velocity of the body is acceleration, then in the work we will use the concept of FMA.

As the initial, we will use the known MM of the current time of the NLFM signal consisting of two LFM fragments with compensation of frequency and phase jumps at their junction for the increasing law of frequency change [10]:

$$\varphi(t)=\begin{cases}2\pi\left[f_0 t+\dfrac{\beta_1 t^2}{2}\right], 0\le t\le T_1;\\ 2\pi\left[(f_0-\delta f_{21})t+\dfrac{\beta_2 t^2}{2}\right]-\delta\varphi_{12}, T_1\le t\le T_{12};\end{cases} \quad (1)$$

where $\beta_1=\dfrac{\Delta f_1}{T_1}$; $\beta_2=\dfrac{\Delta f_2}{T_2}$.

DOI 10.15588/1607-3274-2024-2-3

Input parameters of MM are f_0, T_n, Δf_n. Based on its output parameter $\varphi(t)$ the values of the instantaneous amplitude of the NLFM signal, its spectrum and ACF are calculated from the known relations [1, 2].

2 REVIEW OF THE LITERATURE

The analysis of the studies indicates the widespread use of NLFM signals in various fields of technology [1, 2, 8–19], in particular, radar, sonar, flaw detection, lidar systems, communications, etc. NLFM signals in comparison with LFM signals reduce MPSLL while providing the required range, range measurement accuracy and Doppler frequency shift [11–23].

Many researchers note that there is a potential to further improve the achievable characteristics of NLFM signals due to the structural-parametric optimization of their frequency-time parameters, which can be carried out using the selection method, gradient methods and methods of evolutionary optimization [24–35].

So, in [36], the use of the NLFM signal in a combined system is considered, which involves the simultaneous use of a dedicated frequency range for sensing airspace and communication. The NLFM signal is described as a pulse whose phase change occurs according to a second-order polynomial law. Signal parameters are optimized by selecting phase polynomial coefficients in order to minimize MPSLL. It is noted that the NLFM signal allows you to get better performance by measuring the range and speed of the target compared to the LFM signal and LFM signal with additional weight processing.

In [37], the use of an NLFM signal with a quadratic frequency function is considered in relation to the problem of ultrasonic diagnosis of defects. The results of the experiment showed that the selected NLFM signal provides an optimal ratio of the level of the side lobes and the width of the main lobe of the ACF.

In [38] discusses a hyperbolic frequency modulation signal that is insensitive to Doppler frequency shift. The final parameters of the NLFM signal are obtained using the method of iterative optimization, which is based on the selection of parameters, namely the central frequency and the spectrum width of their sequence.

Various approximations of FM functions (or instantaneous phase changes) are used to conveniently record NLFM MM signals. In [39] discloses a method for describing an NLFM signal based on the use of a stepwise approximation of a phase curve of a hyperbolic frequency modulated signal. To reduce MPSLL simultaneously with the selection of approximation parameters, window processing is used.

A similar approach is used in the study [40] in relation to magnetic-acoustic-electric tomography. A piecewise linear FM function is used, the parameters of which are optimized based on a genetic algorithm.

Another method for reducing MPSLL is based on the synthesis of signals with the desired spectral characteristics, for example, in [41] it is proposed to apply a modified Chebyshev window function to adjust the spectral power density of the signal, which ensures the reduction of MPSLL without high computational complexity.

Reduction of MPSLL can be achieved by synthesizing a new type of signal, as described in [10]. The authors proposed a two-fragment NLFM signal, the first fragment of which has QFM.

3 MATERIALS AND METHODS

We will carry out the development of the MM two-fragment NLFM signal, which consists of LFM and QFM fragments, that is, for the first fragment, the signal frequency changes along the linear. $f_1(t) = F(t)$, for the second – according to the quadratic law $f_2(t) = F(t^2)$.

If the instantaneous frequency of the second portion of the NLFM signal changes in a quadratic law, then the FMR changes linearly in time. For the instantaneous phase, we apply the concept of FMA, which in this case is a constant value:

$$\alpha_2 = \frac{d^3\varphi_2(t)}{dt^3}. \tag{2}$$

Accordingly, the instantaneous frequency of the second fragment:

$$\begin{aligned} f_2(t) &= f_0 + \beta_1 T_1 + \iint_t \alpha_2 dt^2 = \\ &= f_0 + \beta_1 T_1 + \alpha_2\left(\frac{t^2}{2} - T_1 t + \frac{T_1^2}{2}\right). \end{aligned} \tag{3}$$

The resulting expression (3) contains the integration constant, which we find by the relation:

$$C_1 = f_0 + \beta_1 T_1 + \alpha_2 \frac{T_1^2}{2}.$$

Determination of the integration constant is mandatory, since its third component is actually equal to the frequency jump at the junction of the NLFM signal fragments.

In the next step, by integrating (3), we find the instantaneous phase of the second fragment.

$$\varphi_2(t) = 2\pi\left[(f_0 + \beta_1 T_1)t + \alpha_2\left(\frac{t^3}{6} - \frac{T_1}{2}t^2 + \frac{T_1^2}{2}t - \frac{T_1^3}{6}\right)\right]. \tag{4}$$

FMA α_2 is determined using MM input data (1). Based on the fact that:

$$\Delta f_2 = \alpha_2 \iint_{T_2} dt,$$

– FMA α_2 define as:

DOI 10.15588/1607-3274-2024-2-3

$$\alpha_2 = \frac{2\Delta f_2}{T_2^2}. \quad (5)$$

The value (5) is calculated for all expressions.

The considered MM (1) does not take into account the appearance of FMA α_2 at the junction of fragments and its influence on the change in the frequency-time characteristics of the second fragment.

To simplify mathematical expressions, we apply symbols similar to those used in (1):

$$\delta f_{12} = \alpha_2 \frac{t^2}{2}\bigg|_{t=T_1} = \alpha_2 \frac{T_1^2}{2}. \quad (6)$$

Frequency jump (6) causes instantaneous phase jump at fragment junction:

$$\delta\varphi_{12} = 2\pi\alpha_2 \frac{T_1^3}{6}. \quad (7)$$

Like (1) and using (6), (7) we obtain the MM of the current time for the instantaneous phase of the NLFM signal as part of the first LFM and second QFM fragments:

$$\varphi(t) = \begin{cases} 2\pi\left[f_0 t + \frac{\beta_1 t^2}{2}\right], 0 \le t \le T_1; \\ 2\pi\left[\left(f_0 + \beta_1 T_1 - \delta f_{12}\right)t + \frac{\alpha_2 t^2 (t - 3T_1)}{6}\right] - \delta\varphi_{12}, \\ T_1 \le t \le T_{12}. \end{cases} \quad (8)$$

The synthesized MM (8) provides finding the instantaneous phase of the NLFM signal in the current time for the case when the first fragment has LFM and the second QFM. This MM implements an increasing law of frequency change, compensates for phase and frequency jumps at the junction of fragments due to the presence of FMA.

4 EXPERIMENTS

The operability test of the proposed MM two-segment NLFM signals with the first LFM and the second QFM fragments was carried out in the MATLAB software environment.

For experimental studies, the frequency-time parameters of signals that provide observation of their fine structure, namely, instantaneous phase jumps and frequency in oscillograms, were chosen; the nature and number of pulsations of the top of the spectrum, the presence of pulsations on its slopes; MPSLL, the nature of the change in frequency and shape of the SL, the shape and width of the ML ACF.

Fine structure analysis was performed based on the following patterns. The number of ripples of the top of the spectrum and the ripples of the ACF are proportional to the product of the signal deviation by its duration and their values allow us to assess the correspondence of the obtained graphic material to the given parameters. Spectrum breaks, a sharp change in the frequency of pulsations SL ACF and oscillation on the oscillogram indicate the presence of jumps in the instantaneous frequency of the signal. Violation of the oscillogram smoothness, dips in the spectrum, pulsations of its side slopes, changes in the level of SL ACF are a sign of the presence of instantaneous phase jumps of radio frequency oscillations [8, 9].

Based on the results of the fine structure analysis, it is concluded that the obtained results correspond to the specified input parameters of the MM, the adequacy of its work and the reliability of the obtained results.

At the first stage of experimental studies, one-fragment (LFM, QFM) and two-fragment (LFM-LFM, LFM-QFM) signals are compared with equivalent initial frequency, frequency deviation and duration.

Comparative analysis was carried out based on the results of the obtained MRLSS values, its decay rate and width ML ACF of the generated signal at the level of 0.707 of its maximum value.

To determine the advantages of the proposed signal, a group of five LFM-QFM signals was investigated. Since the frequency-time parameters of this group of signals differ, the width of the ML ACF was not measured.

5 RESULTS

The results of modelling single-fragment LFM, QFM and two-fragment LFM-LFM, LFM-QFM signals with equivalent frequency-time parameters are summarized in Table 1.

Table 1 – Results of experimental studies of single-fragment and two-fragment signals

Kind of sign.	T_1. μs	T_2. μs	Δf_1. kHz	Δf_2. kHz	MPSL. dB	Rapid decline. SLL. dB/dec	ML ACF. μs
LFM	120	–	500	–	–13.47	19.75	1.77
QFM	120	–	500	–	–9.08	16.70	1.73
LFM-LFM	20	100	150	350	–18.15	16.0	1.98
LMF-QFM	60	60	100	400	–19.16	25.0	2.17

Analysis of the results of Table 1 indicates that the single-fragment QFM signal has no advantages over the LFM signal. But its useful property is the rounding of the spectrum in the high frequency region.

The above shows Fig. 1 and Fig. 2, which show the spectrum of LFM (Fig. 1a) and QFM (Fig. 2a) signals. The corresponding ACFs are shown in Figure 1b and Figure 2b.

DOI 10.15588/1607-3274-2024-2-3

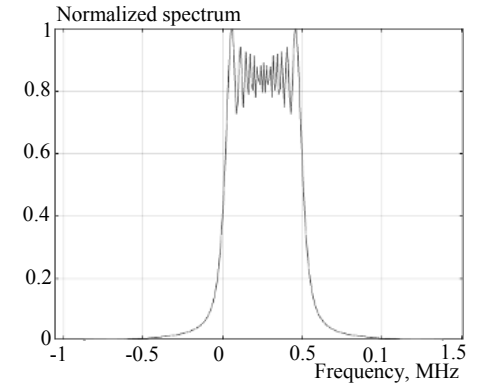

a

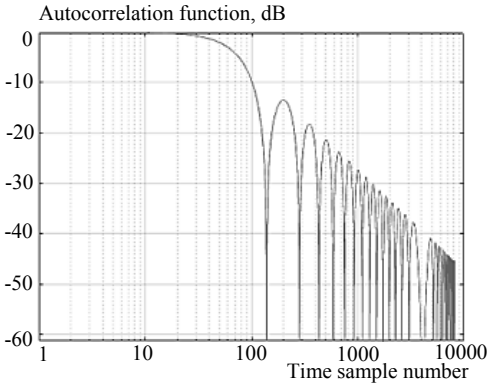

b

Figure 1 – LFM signal: a – spectrum, b – ACF

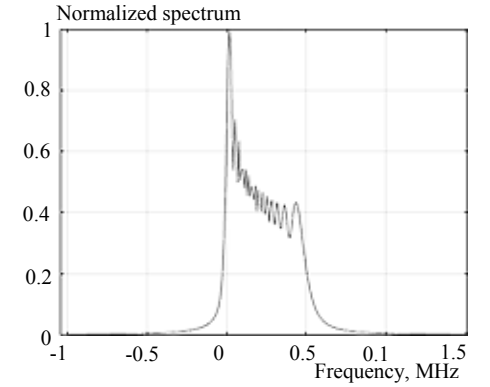

a

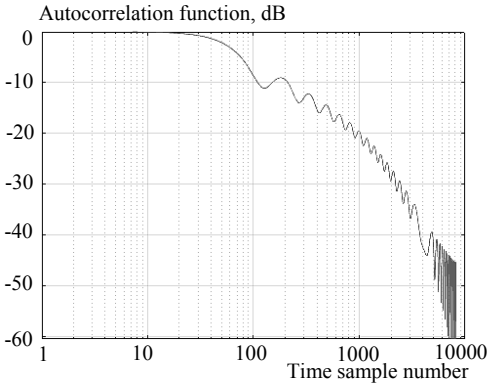

b

Figure 2 – QFM signal: a – spectrum, b – ACF

With regard to two-fragment signals, it should be noted that the main advantage of an NLFM signal with a QFM fragment is a decrease in MPSLL and an increase in the ML ACF decay rate.

The proposed LFM-QFM signal among those shown in Table 1 has the lowest MRSLL, in addition, the width ML of its ACF at the level of 0.707 decreased by 7.5% in relation to the LFM-LFM signal, this leads to an improvement in the range distinguishing ability.

Table 2 shows the results of modelling LFM-QFM signals (8) with different values of time-frequency parameters and corresponding estimates of the obtained indicators.

Table 2 – Results of experimental studies of two-fragment LFM-QFM signals

No.	T_1, μs	T_2, μs	Δf_1, kHz	Δf_2, kHz	MPSL, dB	Rapid decline,SLL dB/dec
1.	60	60	100	350	–19.12	25.0
2.	60	60	100	500	–20.0	26.0
3.	60	60	100	600	–20.46	27.0
4.	80	80	100	600	–20.03	28.0
5.	90	90	100	650	–20.41	29.0

Analysis of the results of Table 2 indicates that the use of the proposed signal provides a decrease in MPLSS (over 2 dB) compared to the LFM-LFM signal. With an increase in the QFM fragment deviation relative to the LFM fragment deviation, with a simultaneous increase in their duration, an increase in MPSLL (by about 1 dB) and an increase in the SL ACF decay rate (by 6 dB/dec) are observed.

Analysis of the fine structure of the LFM-QFM signal with the parameters of Table 1, namely, the frequency change graph, oscillogram, spectrum and ACF shown in Fig. 3, indicates their compliance with the input MM data.

There are no jumps in the instantaneous frequency and phase of the signal at the junction of the fragments, which is confirmed by the appearance of the oscillogram and the signal spectrum. This is evidence that the created MM adequately reproduces the physical processes that occur during the synthesis of LFM-QFM signals and compensates for the manifestations of the action of frequency-phase distortion sources.

It is determined experimentally that stable operation of MM (8) is provided by the ratio of duration of LFM and QFM fragments 1:1 with the step of changing the parameter 20, 30 units. In this case, the frequency deviation can change in increments of 50, 100 units. In the case of equality of frequency deviations of fragments or when the deviation of the LFM fragment is greater, the resulting NLFM signal in its properties approaches the usual LFM signal, which is natural.

Note the peculiarity of the shape of the ACF LFM-QFM signal (Fig. 3g) in comparison with the LFM-LFM (Fig. 4), which must be taken into account, in particular in radar applications.

DOI 10.15588/1607-3274-2024-2-3

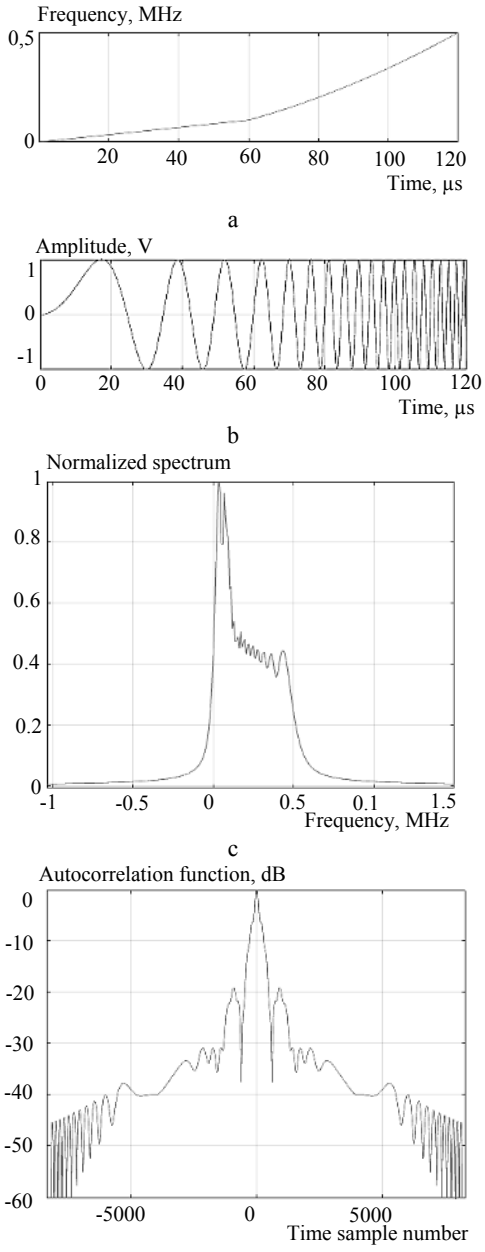

Figure 3 – Signal from LFM-QFM: a – frequency change plot, b – oscillogram, c – spectrum, d – ACF

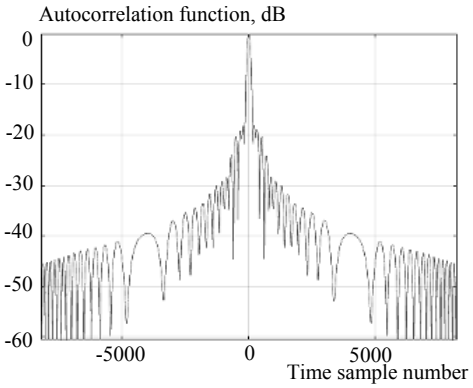

Figure 4 – ACF signal type LFM-LFM

As a result of the merger of ML with near SL, the form of ACF is distorted, at a level of about –10 dB a "pedestal" appears. This form of ACF leads to an increase in the level of the interference background in the presence of long-range interference.

6 DISCUSSION

In works [8, 9], to determine the magnitude of instantaneous phase hopping at the junction of fragments of the NLFM signal, the difference between its value at the beginning of the next fragment and the final value of the previous one was calculated. In this study, a more general approach was used to find analytical expressions of the magnitude of frequency-phase distortions in multifragment NLFM signals, which is based on the calculation of derivatives of the instantaneous phase function of fragments. In this case, the instantaneous frequency (phase) function must have a finite number of derivatives. From this follows the limitation of the list of types of frequency (phase) modulation functions of each of the individual fragments, which is a disadvantage of this approach. Despite this limitation, the application of the proposed approach allowed to substantiate the cause of distortion of the frequency-phase structure at the joints of multifragment NLFM signals. Such a reason is a change in the value of the highest derivative of the instantaneous phase function for fragments with the same FM laws, the appearance of new or possibly the disappearance of existing derivatives if the FM laws of neighboring fragments differ. Thus, the feasibility of further studies is seen, the effect of the disappearance of the existing derivative of the instantaneous phase during the transition to the next fragment on the frequency-phase structure of the resulting signal.

CONCLUSIONS

Scientific novelty. According to the results of the studies, the theory of synthesis of two-fragment signals from NLFM has been developed for the case when the instantaneous phase of one of the signal fragments has the oldest third derivative, and for the other fragment the derivative of the instantaneous phase is limited to the second order. In this case, the source of frequency-phase distortion at the junction of the NLFM signal fragments is FMA (the third derivative of the instantaneous phase).

A new MM NLFM signal of the LFM-QFM type has been developed in the current time, the difference of which is the introduction of an additionals components of the linear and qadratic change in the instantaneous phase of the QFM fragment.

For the synthesized NLFM signal, in comparison with the LFM-LFM signal, the MPSLL value decreased by 2 dB, and its decay rate increased by 9 dB/dec. For the considered group of five such NLFM signals, the MRSLL level varies from –19.12 dB to –20.46 dB, which for two-fragment signals is quite high compared to, for example, [11].

The SLL decay rate of their ACF is within 25 dB/dec – 29 dB/dec, which also exceeds the value of this parame-

DOI 10.15588/1607-3274-2024-2-3

ter for [11], based on the assessment of the given graphic material.

The frequency change graph, oscillogram, spectrum and ACF of the synthesized LFM-QFM signal correspond to the theory and the given parameters, indicating the absence of frequency-phase distortion, which indicates the reliability and adequacy of the developed MM.

The practical significance of the obtained results lies in the possibility of using the proposed approach to the analysis and synthesis on its basis of a wide range of NLFM signals for use as probing in radar devices for various purposes. Experimentally obtained versions of the values of the frequency-time parameters of LFM-QFM signals make it possible to use them in radio electronic systems, in which the value of the range discriminating ability is determining, and passive interference is either absent or their influence can be neglected.

Prospects for further research. In the future, it is planned, using the developed approach, to synthesize MM three-fragment NLFM signals with the resulting FM law close to *S*-shaped.

ACKNOWLEDGEMENTS

We thank the management of Ivan Kozhedub Kharkiv National Air Force University for the opportunity to conduct scientific research.

REFERENCES

1. Levanon N., E. Mozeson Radar Signals [Text]. New York, John Wiley & Sons, 2004, 403 p.
2. Cook C. E., Bernfeld M. Radar Signals: An Introduction to Theory and Application [Text]. Boston, Artech House, 1993, 552 p.
3. Li Tan. Digital Signal Processing. Fundamentals and Applications [Text]. Georgia, Academic Press, 2008, 816 p.
4. Lei T., Liang L. Research and design of digital unit for direct digital frequency synthesizer [Text], *International Conference on Electronic Materials and Information Engineering (EMIE 2021), Journal of Physics: Conference Series,* 2021, Vol. 1907, Article № 012004. DOI:10.1088/1742-6596/1907/1/012004.
5. Genovese M., Napoli E., De Caro D., et al. Analysis and comparison of Direct Digital Frequency Synthesizers implemented on FPGA [Text], *Integration,* 2014, Vol. 47, Issue 2, pp. 261–271.
6. Blackledge J. Digital Signal Processing [Text]. Dublin, Horwood Publishing, second edition, 2006, 840 p.
7. Anil A., Prasad A. FPGA Implementation of DDS for Arbitrary wave generation [Text], *International Journal of Engineering Research and Applications,* 2021, Vol. 11, Issue 7, (Series-II), pp. 56–64. DOI: 10.9790/9622-1107025664.
8. Kostyria O. O., Hryzo A. A., Dodukh O. M. et al. Mathematical model of a two-fragment signal with a non-linear frequency modulation in the current period of time [Text], *Visnyk NTUU KPI Seriia – Radiotekhnika Radioaparatobuduvannia*, 2023, Vol. 92, pp. 60–67. DOI:10.20535/RADAP.2023.92.60-67.
9. Kostyria O. O., Hryzo A. A. , Dodukh O. M. et al. Improvement of mathematical models with time-shift of two- and tri-fragment signals with non-linear frequency modulation [Text], *Visnyk NTUU KPI Seriia – Radiotekhnika Radioaparatobuduvannia,* 2023, Vol. 93, pp. 22–30. DOI: 10.20535/RADAP.2023.93.22-30.
10. Kostyria O. O., Hryzo A. A. , Khizhnyak I. A. et al. Implementation of the Method of Minimizing the Side Lobe Level of Autocorrelation Functions of Signals with Nonlinear Frequency Modulation [Text], V*isnyk NTUU KPI Seriia – Radiotekhnika Radioaparatobuduvannia,* 2024, Vol. 95, pp. 16–22. DOI: 10.20535/RADAP.2024.95.16-22.
11. Anoosha Ch. and Krishna B. T. Peak Side Lobe Reduction analysis of NLFM and Improved NLFM Radar signal with Non-Uniform PRI [Text], *Aiub Journal of Science and Engineering (AJSE),* 2022, Vol. 21, Issue 2, pp. 125–131.
12. Zhaoa Y., Ritchie M., Lua X. et al. Non-continuous piecewise nonlinear frequency modulation pulse with variable sub-pulse duration in a MIMO SAR radar system [Text], *Remote Sensing Letters,* 2020, Vol. 11, Issue 3, pp. 283–292. DOI: 10.1080/2150704X.2019.1711237
13. Valli N. A., Rani D. E., Kavitha C. Modified Radar Signal Model using NLFM [Text], *International Journal of Recent Technology and Engineering (IJRTE),* 2019, Vol. 8, Issue 2S3, pp. 513–516. DOI:10.35940/ijrte.b1091.0782s319
14. Fan Z., Meng H. Coded excitation with Nonlinear Frequency Modulation Carrier in Ultrasound Imaging System [Text], *2020 IEEE Far East NDT New Technology & Application Forum (FENDT). Kunming, Yunnan province.* China, conference paper, IEEE, 2020, pp. 31–35. https://doi.org/10.1109/FENDT50467.2020.9337517.
15. Valli N. A., Rani D. E., Kavitha C. Performance Analysis of NLFM Signals with Doppler Effect and Background Noise [Text], *International Journal of Engineering and Advanced Technology (IJEAT),* 2020, Vol. 9 Issue 3, pp. 737–742. DOI: 10.35940/ijeat.B3835.029320
16. Widyantara M. R., Suratman S.-F. Y., Widodo S. et al. Analysis of nonlinear Frequency Modulation (NLFM) Waveforms for Pulse Compression Radar [Text], *Jurnal Elektronika dan Telekomunikasi,* 2018, Vol. 18, Issue 1, pp. 27–34. DOI: 10.14203/jet.v18.27-34
17. Zhang Y., Deng Y., Zhang Z. et al. Analytic NLFM Waveform Design With Harmonic Decomposition for Synthetic Aperture Radar [Text], *IEEE Geoscience and Remote Sensing Letters,* 2022,Vol. 19, Article no 4513405. DOI: 10.1109/lgrs.2022.3204351
18. Ma H., Wang J., Sun X. et al. Joint Radar-Communication Relying on NLFM-MSK Design [Text], *Wireless Communications and Mobile Computing,* 2022, Vol. Article ID 4711132, 26 p. DOI:10.1155/2022/4711132.
19. Dhawan R., Parihar R., Choudhary A. Multiband dual- and cross-LFM waveform generation using a dual-drive Mach-Sender modulator [Text], *Indian Institute of Technology (IIT),* 2023, 11 p. DOI:10.2139/ssrn.4161569
20. Xu Z., Wang X., Wang Y. Nonlinear Frequency-Modulated Waveforms Modeling and Optimization for Radar Applications [Text], *Mathematics,* 2022, Vol. 10, P. 3939. https://doi.org/10.3390/math10213939.
21. Wang B., Chen X., Li Y.et al. Research on Time Sidelobe Analysis on Pulse Compression Signal [Text] / B. Wang, // *Journal of Physics: 2022 2nd International Conference on Measurement Control and Instrumentation (MCAI 2022), Guangzhou*. China, Conf. Ser., 2022, Vol. 2366. DOI 10.1088/1742-6596/2366/1/012022
22. Saleh M., Omar S.-M., Grivel E. et al. A Variable Chirp Rate Stepped Frequency Linear Frequency Modulation Waveform Designed to Approximate Wideband Non-Linear Radar Waveforms [Text], *Digital Signal Processing,* 2021, Vol. 109, Article №102884. doi 10.1016/j.dsp.2020.102884
23. Swiercz E., Janczak D., Konopko K. Estimation and Classification of NLFM Signals Based on the Tim-Chirp [Text], *Sensors,* 2022,Vol. 22, Issue 21. Article № 8104. DOI: 10.3390/s22218104.
24. Septanto H., Sudjana O., Suprijanto D. A Novel Rule for Designing Tri-Stages Piecewise Linear NLFM Chirp [Text], *2022 International Conference on Radar, Antenna, Microwave, Electronics, and Telecommunications (ICRAMET) 6–7 December*

DOI 10.15588/1607-3274-2024-2-3

2022, proceedings. Bandung, Indonesia, IEEE, 2022, pp. 62–67. DOI:10.1109/ICRAMET56917.2022.9991201.
25. Xie Q., Zeng H., Mo Z. et al. A Two-Step Optimization Framework for Low Sidelobe NLFM Waveform Using Fourier Series [Text], *IEEE Geoscience and Remote Sensing Letters,* 2022, Vol. 19, Article no 4020905. DOI: 10.1109/LGRS.2022.3141081.
26. Jiang T., Li B., Li H. et al. Design and implementation of space borne NLFM radar signal generator [Text], *2nd IYSF Academic Symposium on Artificial Intelligence and Computer Engineering, 1 December 2021: proceedings.* Xi'an, China, 2021, Vol. 12079. DOI:10.1117/12.2623222
27. Van Zyl A. C., Wiehahn E. A., Cillers J. E. et al. Optimised multi-parameter NLFM pulse compression waveform for low time-bandwidth radar [Text], *International Conference on Radar Systems (RADAR 2022),* 2022, pp. 289–294. DOI:10.1049/icp.2022.2332.
28. Singh A. K., Bae K.-B., Park S.-O. NLFM pulse radar for drone detection using predistortion technique [Text], *Journal of Electromagnetic Waves and Applications,* 2021, Vol. 35, Issue 3, pp. 416–429. DOI:10.1080/09205071.2020.1844598
29. Li J. Wang P., Zhang H. et al. A Novel Chaotic-NLFM Signal under Low Oversampling Factors for Deception Jamming Suppression [Text], *Remote Sens.* 2024, Vol. 16, Issue 1. https://doi.org/10.3390/rs16010035
30. Zhuang R., Fan H., Sun Y. et al. Pulse-agile waveform design for nonlinear FM pulses based on spectrum modulation [Text], *IET International Radar Conference,* 2021, pp. 964–969. DOI: 10.1049/icp.2021.0700.
31. Hague D. A. Generating waveform families using multi-tone sinusoidal frequency modulation [Text], *2020 IEEE International Radar Conference (RADAR).* Washington, DC, USA, 2020, pp. 946–951. DOI:10.48550/arXiv.2002.11742
32. Talluri S. R. Effects of High pass Filtering on Transmitted Signals of Non-Linear Frequency Modulated Radar Systems [Text], *International Journal of Advances in Microwave Technology,* 2020, Vol. 4(1), pp. 190–193. DOI:10.32452/IJAMT.2019.190193
33. Shuyi L., Jia Y., Liu Y. et al. Research on Ultra-Wideband NLFM Waveform Synthesis and Grating Lobe Suppression [Text], *Sensors,* 2022, Vol. 22, Issue 24, Article no 9829. https://doi.org/10.3390/s22249829.
34. Mohr C. A., McCormick P. M., Topliff C. A. et al. Gradient-based optimization of PCFM radar waveforms [Text], *IEEE Trans. Aerosp. Electron. Syst.,* 2021, Vol. 57, Issue 2, pp. 935–956. DOI:10.1109/TAES.2020.3037403
35. Roy A., Nemade H. B., Bhattacharjee R. Radar waveform diversity using nonlinear chirp with improved sidelobe level performance [Text], *AEU – International Journal of Electronics and Communications,* 2021, Vol. 136, Article no 153768. DOI: 10.1016/J.AEUE.2021.153768.
36. Mahipathi C., Pardhasaradhi B. P., Gunnery S. et al. Optimum Waveform Selection for Target State Estimation in the Joint Radar-Communication System [Text], *IEEE Open Journal of Signal Processing,* 2024, Vol. 5, pp. 459–477. DOI: 10.1109/OJSP.2024.3359997.
37. Peng S., Jian J., Zhitao L., et al. Nonlinear Frequency Modulation Tfm with Second-Order Tgv and Butterworth Filter for Detection of Cfrp Composites, *Preprint research Paper,* 2024, 12 p. URL: https://ssrn.com/abstract=4747512 or http://dx.doi.org/10.2139/ssrn.4747512.
38. Ping T., Song C., Qi Z. et al. PHS: A Pulse Sequence Method Based on Hyperbolic Frequency Modulation for Speed Measurement [Text], *International Journal of Distributed Sensor Networks,* 2024, Vol. 2024, Article ID 6670576,11 p. DOI:10.1155/2024/6670576
39. Yang J. and Sarkar T. K. A New Doppler-Tolerant Polyphase Pulse Compression Codes Based on Hyperbolic Frequency Modulation [Text], *2007 IEEE Radar Conference: proceedings.* Waltham, MA, USA, IEEE, 2007, pp. 265–270, DOI: 10.1109/RADAR.2007.374225.
40. Cheng Z., Sun Z., Wang J. et al. Magneto-acousto-electrical tomography using nonlinearly frequency-modulated ultrasound [Text], *Physics in Medicine & Biology,* 2024, Vol. 69(8). DOI:10.1088/1361-6560/ad2ee5.
41. Zhang Y., Wang W., Wang R. et al. A Novel NLFM Waveform With Low Sidelobes Based on Modified Chebyshev Window [Text], *IEEE Geoscience and Remote Sensing Letters,* 2020, Vol. 17, No. 5, pp. 814–818. DOI: 10.1109/LGRS.2019.2930817.

Received 06.03.2024.
Accepted 25.04.2024.

УДК 621.396.962

МАТЕМАТИЧНА МОДЕЛЬ ПОТОЧНОГО ЧАСУ СИГНАЛУ З ПОСЛІДОВНИМ ПОЄДНАННЯМ ЛІНІЙНО-ЧАСТОТНО ТА КВАДРАТИЧНО МОДУЛЬОВАНИХ ФРАГМЕНТІВ

Костиря О. О. – д-р техн. наук, с.н.с., провідний науковий співробітник, Харківський національний університет Повітряних Сил імені Івана Кожедуба, Харків, Україна.

Гризо А. А. – канд. техн. наук, доц., начальник науково-дослідної лабораторії, Харківський національний університет Повітряних Сил імені Івана Кожедуба, Харків, Україна.

Худов Г. В. – д-р техн. наук, проф., начальник кафедри Харківський національний університет Повітряних Сил імені Івана Кожедуба, Харків, Україна.

Додух О. М. – канд. техн. наук, провідний науковий співробітник, Харківський національний університет Повітряних Сил імені Івана Кожедуба, Харків, Україна.

Соломоненко Ю. С. – канд. техн. наук, заступник начальника факультету з навчальної та наукової роботи, Харківський національний університет Повітряних Сил імені Івана Кожедуба, Харків, Україна.

АНОТАЦІЯ

Актуальність. Одним з методів вирішення актуальної науково-технічної задачі зниження максимального рівня бічних пелюсток автокореляційних функцій радіолокаційних сигналів є застосування нелінійно-частотно модульованих сигналів. Це забезпечує округлення спектру сигналу, що еквівалентно ваговій (віконній) обробці сигналу у часовій області та може використовуватися спільно з нею. Ряд досліджень сигналів з нелінійною частотною модуляцією, які мають у своєму складі лінійно-частотно модульовані фрагменти, свідчить, що на стику фрагментів виникають спотворення їх частотно-фазової структури. Ці спотворення, у залежності від типу математичної моделі сигналу – поточного або зсунутого часу, викликають у сформованому сигналі відповідно стрибок миттєвої частоти та миттєвої фази або тільки фази. У роботі показано, що стри-

DOI 10.15588/1607-3274-2024-2-3

бки виникають у моменти зміни значення похідної миттєвої фази по закінченні лінійно-частотно модульованого фрагменту. Миттєва частота сигналу, яка є першою похідною миттєвої фази, має тлумачення швидкості обертання вектору сигналу на комплексній площині. Друга похідна миттєвої фази сигналу розуміється як швидкість частотної модуляції. Спотворення цих компонент призводить до появи додаткової складової у лінійному члені миттєвої фази, починаючи з другого фрагменту. Неврахування вказаних частотно-фазових (або тільки фазових) спотворень викликає викривлення спектру результуючого сигналу і, як правило, призводить до зростання максимального рівня бічних пелюсток його автокореляційної функції. Особливості застосування у складних сигналах фрагментів з законами частотної модуляції, які мають різну кількість похідних миттєвої фази сигналу, у відомих роботах не розглядалися, тому дану статтю присвячено цьому питанню.

Мета роботи – розробка математичної моделі поточного часу двофрагментних нелінійно-частотно модульованих сигналів з послідовним поєднанням лінійно-частотно та квадратично модульованих фрагментів, що забезпечує округлення спектру сигналу в області верхніх частот та зниження максимального рівня бічних пелюсток автокореляційної функції і збільшення швидкості його спадання.

Метод. У роботі досліджувалися нелінійно-частотно модульовані сигнали, які складаються з лінійно-частотно та квадратично модульованого фрагментів. За допомогою диференційного аналізу визначався ступінь впливу старшої похідної миттєвої фази на частотно-фазову структуру сигналу. Її зміни оцінювалися за допомогою методів часового та спектрально-кореляційного аналізу. Показники результуючого сигналу, що оцінювалися, – стрибки фази та частоти на стику фрагментів, форма спектру, максимальний рівень бічних пелюсток автокореляційної функції та швидкість їх спадання.

Результати. В статті отримала подальший розвиток теорія синтезу нелінійно-частотно модульованих сигналів. Теоретичний внесок полягає у визначенні нового механізму проявів частотно-фазових спотворень на стику фрагментів та його математичний опис. Встановлено, що при переході від лінійно-частотно модульованого фрагменту до квадратично модульованого першоджерелом частотно-фазових спотворень результуючого сигналу стає третя похідна миттєвої фази, яка за аналогією з теорією руху фізичних тіл є прискоренням частотної модуляції. Наявність цієї похідної призводить до появи нових складових у виразі миттєвої частоти та фази сигналу. Компенсація цих спотворень забезпечує зниження максимального рівня бічних пелюсток на 5 дБ та збільшення швидкості його спадання на 8 дБ/дек для розглянутого варіанту нелінійно-частотно модульованого сигналу.

Висновки. Розроблено нову математичну модель поточного часу для розрахунку значень миттєвої фази нелінійно-частотно модульованого сигналу, перший фрагмент якого має лінійну, а другий – квадратичну частотну модуляцію. Відмінністю цієї моделі від відомих є введення нових складових, які забезпечують компенсацію частотно-фазових спотворень на стику фрагментів та у фрагменті з квадратичною частотною модуляцією. Отримані осцилограма, спектр та автокореляційна функція одного з синтезованих двофрагментних сигналів відповідають теоретичному вигляду, що свідчить про адекватність та достовірність запропонованої математичної моделі.

КЛЮЧОВІ СЛОВА: математична модель; лінійна та квадратична частотна модуляція; максимальний рівень бічних пелюсток.

ЛІТЕРАТУРА

1. Levanon N. Radar Signals [Text] / N. Levanon, E. Mozeson. – New York : John Wiley & Sons, 2004. – 403 p.
2. Cook C. E. Radar Signals: An Introduction to Theory and Application [Text] / C. E. Cook, M. Bernfeld. – Boston : Artech House, 1993. – 552 p.
3. Li Tan Digital Signal Processing. Fundamentals and Applications [Text] / Li Tan. – Georgia : Academic Press, 2008. – 816 p.
4. Lei T. Research and design of digital unit for direct digital frequency synthesizer [Text] / T. Lei, L. Liang // International Conference on Electronic Materials and Information Engineering (EMIE 2021), Journal of Physics: Conference Series, 2021. – Vol. 1907. – Article № 012004. DOI:10.1088/1742-6596/1907/1/012004.
5. Analysis and comparison of Direct Digital Frequency Synthesizers implemented on FPGA [Text] / [M. Genovese, E. Napoli, D. De Caro et al.] // Integration. – 2014. – Vol. 47, Issue 2. – P. 261–271.
6. Blackledge J. Digital Signal Processing [Text] / J. Blackledge. – Dublin : Horwood Publishing, second edition, 2006. – 840 p.
7. Anil A. FPGA Implementation of DDS for Arbitrary wave generation [Text] / A. Anil, A. Prasad // International Journal of Engineering Research and Applications. – 2021. – Vol. 11, Issue 7, (Series-II). – P. 56–64. DOI: 10.9790/9622-1107025664.
8. Mathematical model of a two-fragment signal with a non-linear frequency modulation in the current period of time [Text] / [O. O. Kostyria, A. A. Hryzo, O. M. Dodukh et al.] // Visnyk NTUU KPI Seriia – Radiotekhnika Radioaparatobuduvannia. – 2023. – Vol. 92. – P. 60–67. DOI:10.20535/RADAP.2023.92.60-67.
9. Improvement of mathematical models with time-shift of two- and tri-fragment signals with non-linear frequency modulation [Text] / [O. O. Kostyria, A. A. Hryzo, O. M. Dodukh et al.] // Visnyk NTUU KPI Seriia – Radiotekhnika Radioaparatobuduvannia. – 2023. – Vol. 93. – P. 22–30. DOI: 10.20535/RADAP.2023.93.22-30.
10. Implementation of the Method of Minimizing the Side Lobe Level of Autocorrelation Functions of Signals with Nonlinear Frequency Modulation [Text] / [O. O. Kostyria, A. A. Hryzo, I. A. Khizhnyak et al.] // Visnyk NTUU KPI Seriia – Radiotekhnika Radioaparatobuduvannia. – 2024. – Vol. 95. – P. 16–22. DOI: 10.20535/RADAP.2024.95.16-22.
11. Anoosha Ch. Peak Side Lobe Reduction analysis of NLFM and Improved NLFM Radar signal with Non-Uniform PRI [Text] / Ch Anoosha and B. T. Krishna // Aiub Journal of Science and Engineering (AJSE). – 2022. – Vol. 21, Issue 2. – P. 125–131.
12. Non-continuous piecewise nonlinear frequency modulation pulse with variable sub-pulse duration in a MIMO SAR radar system [Text] / [Y. Zhaoa, M. Ritchie, X. Lua et al.] // Remote Sensing Letters. – 2020. – Vol. 11, Issue 3. – P. 283–292. DOI: 10.1080/2150704X.2019.1711237
13. Valli N. A. Modified Radar Signal Model using NLFM [Text] / N. A. Valli, D. E. Rani, C. Kavitha // International Journal of Recent Technology and Engineering (IJRTE). – 2019. – Vol. 8, Issue 2S3. – P. 513–516. DOI:10.35940/ijrte.b1091.0782s319
14. Fan Z. Coded excitation with Nonlinear Frequency Modulation Carrier in Ultrasound Imaging System [Text] / Z. Fan, H. Meng // 2020 IEEE Far East NDT New Technology & Application Forum (FENDT). Kunming, Yunnan province, China : conference paper. IEEE. – 2020. – P. 31–35. https://doi.org/10.1109/FENDT50467.2020.9337517.
15. Valli N. A. Performance Analysis of NLFM Signals with Doppler Effect and Background Noise [Text] / N. A. Valli, D. E. Rani, C. Kavitha // International Journal of Engineering

DOI 10.15588/1607-3274-2024-2-3

and Advanced Technology (IJEAT). – 2020. – Vol. 9, Issue 3. – P. 737–742. DOI: 10.35940/ijeat.B3835.029320
16. Analysis of nonlinear Frequency Modulation (NLFM) Waveforms for Pulse Compression Radar [Text] / [M. R. Widyantara, S.-F. Y. Suratman, S. Widodo et al.] // Jurnal Elektronika dan Telekomunikasi. – 2018. – Vol. 18, Issue 1. – P. 27–34. DOI: 10.14203/jet.v18.27-34
17. Analytic NLFM Waveform Design With Harmonic Decomposition for Synthetic Aperture Radar [Text] / [Y. Zhang, Y. Deng, Z. Zhang et al.] // IEEE Geoscience and Remote Sensing Letters. – 2022. – Vol. 19, Article no 4513405. doi:10.1109/lgrs.2022.3204351
18. Joint Radar-Communication Relying on NLFM-MSK Design [Text] / [H. Ma, J. Wang, X. Sun et al.] // Wireless Communications and Mobile Computing. – 2022. – Vol. Article ID 4711132, 26 p. DOI:10.1155/2022/4711132.
19. Dhawan R. Multiband dual- and cross-LFM waveform generation using a dual-drive Mach-Sender modulator [Text] / R. Dhawan, R. Parihar, A. Choudhary // Indian Institute of Technology (IIT), 2023. – 11 p. DOI:10.2139/ssrn.4161569
20. Xu Z. Nonlinear Frequency-Modulated Waveforms Modeling and Optimization for Radar Applications [Text] / Z. Xu, X. Wang, Y Wang // Mathematics. – 2022. – Vol. 10. – P. 3939. https://doi.org/10.3390/math10213939.
21. Research on Time Sidelobe Analysis on Pulse Compression Signal [Text] / [B. Wang, X. Chen, Y. Li et al.] // Journal of Physics: 2022 2nd International Conference on Measurement Control and Instrumentation (MCAI 2022), Guangzhou, China. Conf. Ser. – 2022. – Vol. 2366. DOI 10.1088/1742-6596/2366/1/012022
22. A Variable Chirp Rate Stepped Frequency Linear Frequency Modulation Waveform Designed to Approximate Wideband Non-Linear Radar Waveforms [Text] / [M. Saleh, S.-M. Omar, E. Grivel et al.] // Digital Signal Processing. – 2021. – Vol. 109. – Article №102884. DOI 10.1016/j.dsp.2020.102884
23. Swiercz E. Estimation and Classification of NLFM Signals Based on the Time-Chirp [Text] / E. Swiercz, D. Janczak, K. Konopko // Sensors. – 2022. – Vol. 22, Issue 21. Article № 8104. doi: 10.3390/s22218104.
24. Septanto H. A Novel Rule for Designing Tri-Stages Piecewise Linear NLFM Chirp [Text] / H. Septanto, O. Sudjana, D. Suprijanto // 2022 International Conference on Radar, Antenna, Microwave, Electronics, and Telecommunications (ICRAMET) 6–7 December 2022: proceedings. – Bandung, Indonesia : IEEE, 2022. – P. 62–67. DOI:10.1109/ICRAMET56917.2022.9991201.
25. A Two-Step Optimization Framework for Low Sidelobe NLFM Waveform Using Fourier Series [Text] / [Q. Xie, H. Zeng, Z. Mo et al.] // IEEE Geoscience and Remote Sensing Letters. – 2022. – Vol. 19, Article no 4020905. DOI: 10.1109/LGRS.2022.3141081.
26. Design and implementation of space borne NLFM radar signal generator [Text] / [T. Jiang, B. Li, H. Li et al.] // 2nd IYSF Academic Symposium on Artificial Intelligence and Computer Engineering, 1 December 2021: proceedings. – Xi'an, China. – 2021. – Vol. 12079. doi:10.1117/12.2623222
27. Optimised multi-parameter NLFM pulse compression waveform for low time-bandwidth radar [Text] / [A. C. van Zyl, E. A. Wiehahn, J. E. Cillers et al.] // International Conference on Radar Systems (RADAR 2022). – 2022. – P. 289–294. DOI:10.1049/icp.2022.2332.
28. Singh A. K. NLFM pulse radar for drone detection using predistortion technique [Text] / A. K. Singh, K.-B. Bae, S.-O. Park // Journal of Electromagnetic Waves and Applications, 2021. – Vol. 35, Issue 3. – P. 416–429. doi:10.1080/09205071.2020.1844598
29. A Novel Chaotic-NLFM Signal under Low Oversampling Factors for Deception Jamming Suppression [Text] / [J. Li, P. Wang, H. Zhang et al.] // Remote Sens. 2024. – Vol. 16, Issue 1. https://doi.org/10.3390/rs16010035
30. Pulse-agile waveform design for nonlinear FM pulses based on spectrum modulation [Text] / [R. Zhuang, H. Fan, Y. Sun et al.] // IET International Radar Conference. – 2021. – P. 964–969. DOI: 10.1049/icp.2021.0700.
31. Hague D. A. Generating waveform families using multi-tone sinusoidal frequency modulation [Text] / D. A. Hague // 2020 IEEE International Radar Conference (RADAR): Washington, DC, USA, 2020. – P. 946–951. DOI:10.48550/arXiv.2002.11742
32. Talluri S. R. Effects of High pass Filtering on Transmitted Signals of Non-Linear Frequency Modulated Radar Systems [Text] / S. R. Talluri // International Journal of Advances in Microwave Technology. – 2020. – Vol. 4(1). – P. 190–193. DOI:10.32452/IJAMT.2019.190193
33. Research on Ultra-Wideband NLFM Waveform Synthesis and Grating Lobe Suppression [Text] / [L. Shuyi, Y. Jia, Y. Liu et al.] // Sensors. – 2022. – Vol. 22, Issue 24. – Article no 9829. https://doi.org/10.3390/s22249829.
34. Gradient-based optimization of PCFM radar waveforms [Text] / [C. A. Mohr, P. M. McCormick, C. A. Topliff et al.] // IEEE Trans. Aerosp. Electron. Syst. – 2021. – Vol. 57, Issue 2. – P. 935–956. DOI:10.1109/TAES.2020.3037403
35. Roy A. Radar waveform diversity using nonlinear chirp with improved sidelobe level performance [Text] / A. Roy, H. B. Nemade, R. Bhattacharjee // AEU – International Journal of Electronics and Communications. – 2021. – Vol. 136. – Article no 153768. DOI: 10.1016/J.AEUE.2021.153768.
36. Optimum Waveform Selection for Target State Estimation in the Joint Radar-Communication System [Text] / [C. Mahipathi, B. P. Pardhasaradhi, S. Gunnery et al.] // IEEE Open Journal of Signal Processing, 2024. – Vol. 5. – P. 459–477. DOI: 10.1109/OJSP.2024.3359997.
37. Nonlinear Frequency Modulation Tfm with Second-Order Tgv and Butterworth Filter for Detection of Cfrp Composites / [S. Peng, J. Jian, L. Zhitao, et al.] // Preprint research Paper, 2024. – 12 p. URL: https://ssrn.com/abstract=4747512 or http://dx.doi.org/10.2139/ssrn.4747512.
38. PHS: A Pulse Sequence Method Based on Hyperbolic Frequency Modulation for Speed Measurement [Text] / [T. Ping, C. Song, Z. Qi et al.] // International Journal of Distributed Sensor Networks. – 2024. – Vol. 2024, Article ID 6670576. – 11 p. doi:10.1155/2024/6670576
39. Yang J. A New Doppler-Tolerant Polyphase Pulse Compression Codes Based on Hyperbolic Frequency Modulation [Text] / J. Yang and T. K. Sarkar // 2007 IEEE Radar Conference: proceedings. – Waltham, MA, USA: IEEE, 2007. – P. 265–270. DOI: 10.1109/RADAR.2007.374225.
40. Cheng Z. Magneto-acousto-electrical tomography using nonlinearly frequency-modulated ultrasound [Text] / [Z. Cheng, Z. Sun, J. Wang et al.]. // Physics in Medicine & Biology. – 2024. – Vol. 69(8). DOI: 10.1088/1361-6560/ad2ee5.
41. A Novel NLFM Waveform With Low Sidelobes Based on Modified Chebyshev Window [Text] / [Y. Zhang, W. Wang, R. Wang et al.] // IEEE Geoscience and Remote Sensing Letters. – 2020. – Vol. 17, No. 5. – P. 814–818. DOI: 10.1109/LGRS.2019.2930817.

DOI 10.15588/1607-3274-2024-2-3